

Seasonal Rainfall Analyses over Lake Tana: Teleconnection and Prediction

○Asmaa ALHAMSHRY, Ayele A. FENTA, Hiroshi YASUDA, Reiji KIMURA,
Takayuki KAWAI, Katsuki SHIMIZU

1. Introduction and objectives:

Summer rainfall (June–September) accounts for about 80% of the annual rainfall in the Lake Tana basin of Ethiopia (Fig. 1), the source region of the Blue Nile River which contributes about 60% of the Nile River flow at Aswan High Dam, Egypt (Taye and Willems 2012). Prediction of summer rainfall would be valuable for managing the region's water resources and agricultural operations.

This study investigated the influence of sea surface temperature (SST) as a predictor of summer rainfall in the basin by applying cross-correlation analysis between summer rainfall and climatic indices and SST in various oceanic regions from 1985 to 2015 (30 years).



Fig. 1 Location map of Lake Tana in Ethiopia

2. Methods and Data:

In 2011, Diro et al. indicated that the statistical method of prediction relies on linkages between rainfall and climate parameters, of which SST is the key predictor because it changes slowly and is strongly coupled to the atmosphere. Therefore, in this study, we sought to develop a predictive model for summer rainfall in the Lake Tana basin by identifying the oceanic regions for which their SSTs have strong teleconnections to summer rainfall.

For this purpose, we applied a neural network model to evaluate predictions of summer rainfall from SSTs in these oceanic regions at useful lead times.

This process began by evaluating teleconnections to various climatic indices, then by analyzing the components of the most promising indices.

To achieve our objectives, we considered three sets of data. The first set is the monthly rainfall data covering the period 1985–2015 from the satellite estimates in the Climate Hazards group Infrared Rainfall with Station (CHIRPS) dataset version 2, with a spatial resolution of 5 km, the second set is Global SST data were obtained from Hadley Centre Global Sea Ice and Sea Surface Temperature (HadISST) version 1.1 by the British Atmospheric Data Center. This product gives monthly mean temperatures with a resolution of $1^\circ \times 1^\circ$ for the period 1984–2015 (1 year more than the rainfall data), considering lag months, and the third set is the six climatic indices (PDO, IOD, SOI, NAO, MOI, AO).

3. Results and discussions:

The mean annual rainfall in the study area is 1272 mm, of which 1024 mm or 80.5% occurs in the summer rainfall season. Rainfall is mainly concentrated from June to September and is greatest in July and August, corresponding with the lowest coefficient of variation (Fig. 2).

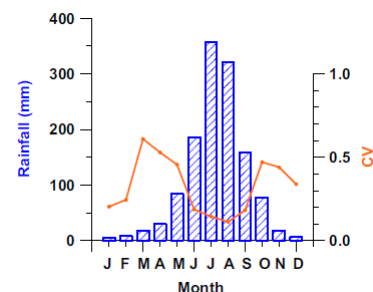


Fig. 2 Monthly average rainfall and coefficient of variation (CV) of rainfall in the study area

When normalized with respect to the long-term (1985–2015) average, the annual summer rainfall tended to alternate between dry and wet years between 1985 and 1998 and to vary randomly between dry and wet in later years (Fig. 3). This record emphasizes the high spatial variability of rainfall in the Lake Tana basin due to its complex topographic and geographic setting.

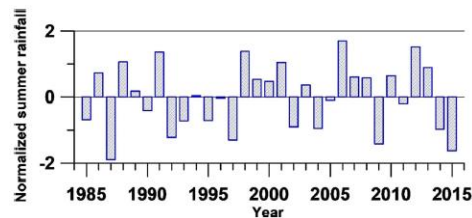


Fig. 3 Summer rainfall in the study area normalized with respect to the 1985–2015 average

Summer rainfall analysis showed a strong negative correlation (-0.665) with the Pacific Decadal Oscillation index at short time lags (Fig. 4).

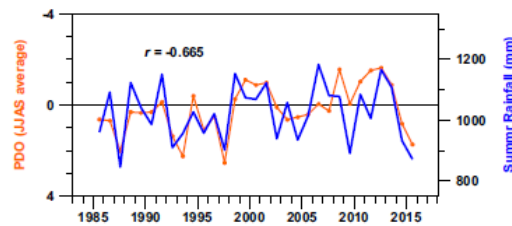


Fig. 4 Time series of the average PDO index for JJAS (lag of 0 month) and summer rainfall in the study area

Further analysis identified strong teleconnections ($|r| \geq 0.5$) between SSTs in specific parts of the Pacific Ocean and summer rainfall in the Lake Tana basin, raising the possibility of predicting summer rainfall from Pacific SSTs with a lead time of 4 to 5 months (Fig. 5).

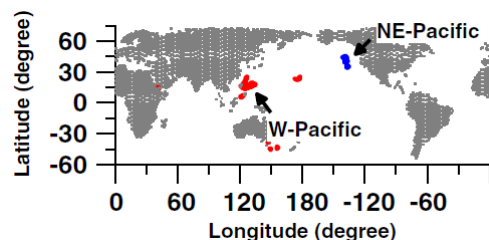


Fig. 5 Common regions of the Pacific Ocean that are strongly correlated with summer rainfall in the study area at lags of both 4 and 5 months

Average SSTs of an area near the Philippines and an area west of North America were positively correlated (0.629) and negatively correlated (-0.538), respectively, with summer rainfall in the Lake Tana basin (Fig. 6).

Predictions of summer rainfall from these teleconnected SSTs by an Elman recurrent neural network model were encouraging, indicating a strong correlation ($r > 0.77$) between the observed and predicted summer rainfall (Fig. 7).

This study demonstrated that our neural network model is skillful enough to provide the basis of seasonal rainfall predictions over the basin of Lake Tana in Ethiopia, a prerequisite for early drought

warnings and accurate water allocation among the nations that rely on the Nile River. To expand the scale from the basin size to country wide, the meteorological property is not homogenous. Therefore, zoning could be essential for large-scale analysis.

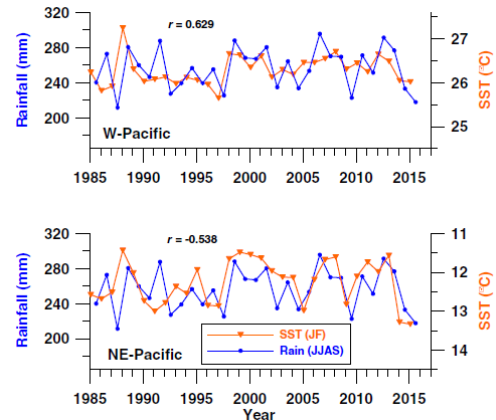


Fig. 6 Time series showing summer rainfall in the study area and January–February SST of Pacific regions located in (Fig. 5)

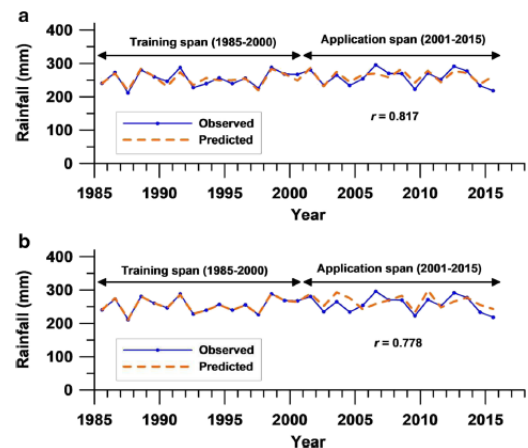


Fig. 7 Time series of observed summer rainfall in the study area and corresponding rainfall predicted by the neural network from SST in the regions of W-Pacific (a) and NE-Pacific (b) as located in (Fig. 5)

References:

- (1) Diro GT, Grimes DIF, Black E (2011a): Teleconnections between Ethiopian summer rainfall and sea surface temperature: part I. Observation and modeling. *Clim Dyn* 37(1):121–131. <https://doi.org/10.1007/s00382-010-0837-8>.
- (2) Taye MT, Willems P (2012): Temporal variability of hydroclimatic extremes in the Blue Nile basin. *Water Resour Res* 48(3):1–13. <https://doi.org/10.1029/2011WR011466>.

Abbreviations

PDO	Pacific Decadal Oscillation
IOD	Indian Ocean Dipole
SOI	Southern Oscillation Index
NAO	North Atlantic Oscillation
MOI	Mediterranean Oscillation Index
AO	Arctic Oscillation
JJAS	June July August September

The study was published as;

Alhamshry, Asmaa, et al. "Prediction of summer rainfall over the source region of the Blue Nile by using teleconnections based on sea surface temperatures." *Theoretical and Applied Climatology* 137 (2019): 3077–3087.